Cell, Vol. 115, 199–208, October 17, 2003, Copyright ©2003 by Cell Press

Asymmetry in the Assembly of the RNAi Enzyme Complex

Dianne S. Schwarz,[1,3] György Hutvágner,[1,3] Tingting Du,[1] Zuoshang Xu,[1] Neil Aronin,[2] and Phillip D. Zamore[1,*]
[1]Department of Biochemistry and Molecular Pharmacology and
[2]Department of Medicine
University of Massachusetts Medical School
Lazare Research Building
364 Plantation Street
Worcester, Massachusetts 01605

Summary

A key step in RNA interference (RNAi) is assembly of the RISC, the protein-siRNA complex that mediates target RNA cleavage. Here, we show that the two strands of an siRNA duplex are not equally eligible for assembly into RISC. Rather, both the absolute and relative stabilities of the base pairs at the 5′ ends of the two siRNA strands determine the degree to which each strand participates in the RNAi pathway. siRNA duplexes can be functionally asymmetric, with only one of the two strands able to trigger RNAi. Asymmetry is the hallmark of a related class of small, single-stranded, noncoding RNAs, microRNAs (miRNAs). We suggest that single-stranded miRNAs are initially generated as siRNA-like duplexes whose structures predestine one strand to enter the RISC and the other strand to be destroyed. Thus, the common step of RISC assembly is an unexpected source of asymmetry for both siRNA function and miRNA biogenesis.

Introduction

Two types of ~21 nt RNAs trigger posttranscriptional gene silencing in animals: small interfering RNAs (siRNAs) and microRNAs (miRNAs). Both siRNAs and miRNAs are produced by the cleavage of double-stranded RNA (dsRNA) precursors by Dicer, a member of the RNase III family of dsRNA-specific endonucleases (Bernstein et al., 2001; Billy et al., 2001; Grishok et al., 2001; Hutvágner et al., 2001; Ketting et al., 2001; Knight and Bass, 2001; Paddison et al., 2002; Park et al., 2002; Provost et al., 2002; Reinhart et al., 2002; Zhang et al., 2002; Doi et al., 2003; Myers et al., 2003). siRNAs result when transposons, viruses, or endogenous genes express long dsRNA or when dsRNA is introduced experimentally into plant or animal cells to trigger gene silencing, a process known as RNA interference (RNAi) (Fire et al., 1998; Hamilton and Baulcombe, 1999; Zamore et al., 2000; Elbashir et al., 2001a; Hammond et al., 2001; Sijen et al., 2001; Catalanotto et al., 2002). In contrast, miRNAs are the products of endogenous, noncoding genes whose precursor RNA transcripts can form small stem loops from which mature miRNAs are cleaved by Dicer (Lagos-Quintana et al., 2001, 2002, 2003; Lau et al., 2001; Lee and Ambros, 2001; Mourelatos et al., 2002; Reinhart et al., 2002; Ambros et al., 2003; Brennecke et al., 2003; Lim et al., 2003a, 2003b). miRNAs are encoded in genes distinct from the mRNAs whose expression they control.

siRNAs were first identified as the specificity determinants of the RNAi pathway, where they act as guides to direct endonucleolytic cleavage of their target RNAs (Hamilton and Baulcombe, 1999; Hammond et al., 2000; Zamore et al., 2000; Elbashir et al., 2001a). Prototypical siRNA duplexes are 21 nt double-stranded RNAs that contain 19 base pairs, with 2 nt, 3′ overhanging ends (Elbashir et al., 2001a; Nykänen et al., 2001; Tang et al., 2003). Active siRNAs, like miRNAs, contain 5′ phosphates and 3′ hydroxyls (Zamore et al., 2000; Boutla et al., 2001; Hutvágner et al., 2001; Nykänen et al., 2001; Chiu and Rana, 2002; Mallory et al., 2002). Recent evidence suggests that siRNAs and miRNAs are functionally interchangeable, with the choice of mRNA cleavage or translational repression determined solely by the degree of complementarity between the small RNA and its target (Hutvágner and Zamore, 2002; Doench et al., 2003; Zeng and Cullen, 2003). siRNAs and miRNAs are found in similar, if not identical, complexes, suggesting that a single, bifunctional complex—the RNA-induced silencing complex (RISC)—mediates both cleavage and translational control (Caudy et al., 2002; Hutvágner and Zamore, 2002; Martinez et al., 2002; Mourelatos et al., 2002).

Each RISC contains only one of the two strands of the siRNA duplex (Martinez et al., 2002). Both siRNA strands can be competent to direct RNAi (Elbashir et al., 2001a, 2001b; Nykänen et al., 2001). That is, the anti-sense strand of an siRNA can direct cleavage of a corresponding sense RNA target, whereas the sense siRNA strand directs cleavage of an anti-sense target. Here, we show that small changes in siRNA sequence have profound and predictable effects on the extent to which the individual strands of an siRNA duplex enter the RNAi pathway, a phenomenon we term siRNA functional asymmetry. We designed siRNAs that are fully asymmetric, with only one of the two siRNA strands forming RISC in vitro. Such highly asymmetric siRNA duplexes resemble intermediates previously proposed for the miRNA biogenesis pathway (Hutvágner and Zamore, 2002; Reinhart et al., 2002; Lim et al., 2003b). Our data suggest that RISC assembly is governed by an enzyme that selects which strand of an siRNA is loaded into RISC. This strand is always the one whose 5′ end is less tightly paired to its complement. We propose that for each siRNA duplex that is unwound, only one strand enters the RISC complex, whereas the other strand is degraded. For miRNAs, it is the miRNA strand of a short-lived, siRNA duplex-like intermediate that assembles into a RISC complex, causing miRNAs to accumulate in vivo as single-stranded RNAs. Designing siRNAs to be more like these double-stranded miRNA intermediates produces highly functional siRNAs, even when targeting mRNA sequences apparently refractory to cleavage by siRNAs selected by conventional siRNA design rules.

*Correspondence: phillip.zamore@umassmed.edu
[3]These authors contributed equally to this work.

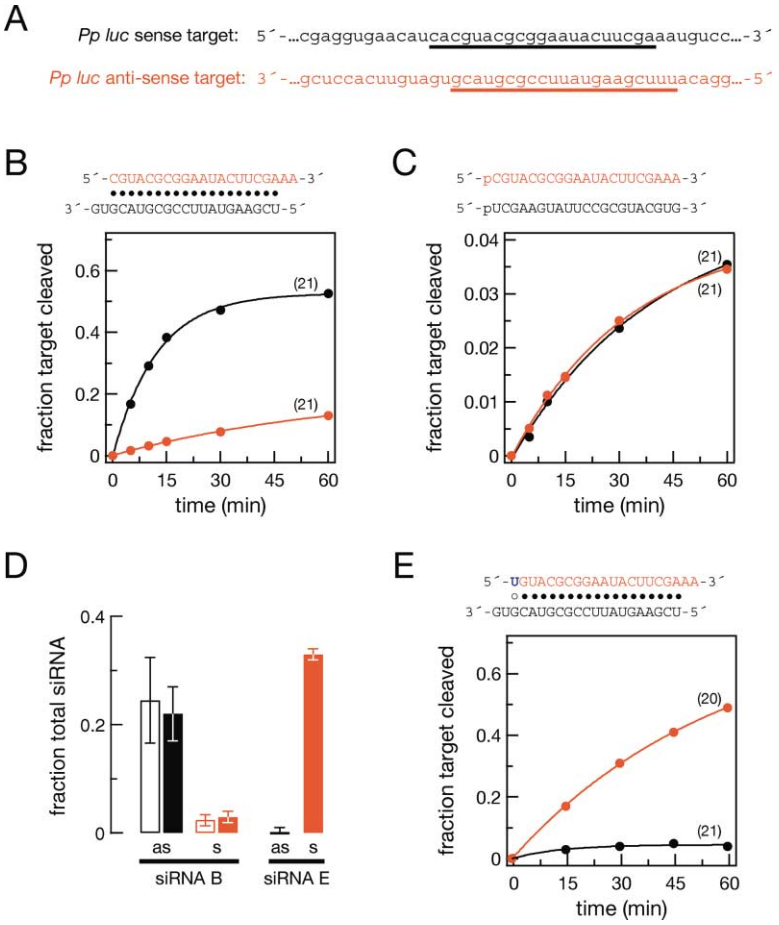

Figure 1. The Two Strands of an siRNA Duplex Do Not Equally Populate the RISC

(A) Firefly luciferase sense and anti-sense target RNA sequences.

(B) In vitro RNAi reactions programmed with the siRNA duplex indicated above the graph.

(C) In vitro RNAi reactions as in (B) but programmed with either the anti-sense or sense single-stranded, 5′ phosphorylated siRNAs indicated above the graph.

(D) Fraction of anti-sense (black) and sense (red) siRNA strands assembled into RISC (open columns) or present as single strands (filled columns) after incubation with *Drosophila* embryo lysate for the siRNA duplexes shown in (B) and (E). The average of four trials ± standard deviation is shown.

(E) In vitro RNAi reactions programmed with the siRNA duplex indicated above the graph and the target RNAs in (A). Throughout the figures, the number of Watson-Crick base pairs formed between the siRNA guide strand and the target RNA is indicated in parentheses, and siRNA bases that mismatch with the target RNA are noted in blue.

Results and Discussion

Functionally Asymmetric siRNA Duplexes

To assess if the two strands of an siRNA duplex are equally competent to direct RNAi, we measured the in vitro rates of sense and anti-sense target cleavage for an siRNA duplex directed against firefly luciferase mRNA (Figure 1A). For this siRNA, the anti-sense siRNA strand directed more-efficient RNAi against its sense target RNA than the sense siRNA strand did toward the anti-sense target (Figure 1B). (Throughout this paper, anti-sense siRNA strands and their sense target RNAs are presented in black and sense siRNAs and their anti-sense targets in red.) Control experiments showed that using siRNA duplexes with 5′ phosphates did not alter this result (data not shown), indicating that different rates of 5′ phosphorylation for the two strands cannot explain the asymmetry.

Single-stranded siRNA can direct RNAi but is >10-fold less effective than siRNA duplexes, reflecting the reduced stability of single-stranded RNA in vitro and in vivo (Schwarz et al., 2002). Surprisingly, the two strands of the luciferase siRNA duplex, used individually as 5′ phosphorylated single-strands, had identical rates of target cleavage (Figure 1C). Thus, the difference in the cleavage rates of the sense and anti-sense strands cannot reflect a difference in the inherent susceptibility of the two targets to RNAi. Instead, the finding that the two siRNA strands are equally effective as single strands but show dramatically different activities when paired to each other suggests that the asymmetry in their function is established at a step in the RNAi pathway before the encounter of the programmed RISC with its RNA target.

Differential RISC Assembly and siRNA Functional Asymmetry

siRNA unwinding correlates with siRNA function (Nykänen et al., 2001; Martinez et al., 2002), likely because siRNA duplex unwinding is required to assemble a RISC competent to base pair with its target RNA. We measured the accumulation of single-stranded siRNA from the luciferase siRNA duplex after 1 hr incubation in an in vitro RNAi reaction in the absence of target RNA. In this reaction, ~22% of the anti-sense strand of the luciferase siRNA was converted to single-strand (Figure 1D, siRNA B, solid black bar). Remarkably, we did not detect a corresponding amount of single-stranded sense siRNA (Figure 1D, siRNA B, solid red bar). Since the production of single-stranded anti-sense siRNA must be accompanied by an equal amount of single-stranded sense siRNA, the missing sense strand must have been destroyed after unwinding.

We also used a novel RISC-capture assay to measure the fraction of each siRNA strand that was assembled into RISC (G.H., M. Simard, C. Mello, and P.D.Z., unpub-

lished data). Double-stranded siRNA was incubated in an RNAi reaction for 1 hr, then we added a complementary 2′-*O*-methyl oligonucleotide tethered to a magnetic bead via a biotin-streptavidin linkage. 2′-*O*-methyl oligonucleotides are not cleaved by the RNAi machinery but can bind stably to complementary siRNA within the RISC, so the amount of radioactivity stably associated with the beads is a direct measure of the amount of RISC formed. The assay was performed with siRNA duplexes in which either the sense or the anti-sense strand was 5′-^{32}P-radiolabeled. All RISC activity directed by the siRNA strand complementary to the tethered oligonucleotide was captured on the beads; no RISC was captured by an unrelated 2′-*O*-methyl oligonucleotide (data not shown). The RISC-capture assay recapitulated our unwinding measurements: ten-fold more anti-sense siRNA-containing RISC was detected than sense-strand RISC (Figure 1D, siRNA B, open bars). The simplest explanation is that the two strands of the siRNA duplex are differentially loaded into the RISC and that single-stranded siRNA not assembled into RISC is degraded.

siRNA Structure and RISC Assembly

The finding that the two siRNA strands can have different capacities to form RISC when paired suggests that some feature unique to the duplex determines functional asymmetry. For the siRNA in Figure 1B, the 5′ end of the anti-sense siRNA strand begins with U and is thus paired to the sense siRNA strand by an U:A base pair (two hydrogen bonds). In contrast, the 5′ nucleotide of the sense siRNA strand is linked to the anti-sense strand by a C:G base pair (three hydrogen bonds). A simple hypothesis is that the siRNA strand whose 5′ end is more weakly bound to the complementary strand more readily incorporates into RISC.

As an initial test of this idea, we changed the first nucleotide of the siRNA sense strand from C to U, replacing a C:G pair with a less stable U:G wobble. The sequence of the anti-sense siRNA was not altered (Figure 1E). This single nucleotide substitution increased the rate of cleavage directed by the sense strand and virtually eliminated RNAi directed by the anti-sense strand (Figure 1E). That is, the single C-to-U substitution inverted the functional asymmetry of the siRNA. Assembly of the two strands of the siRNA into RISC was also reversed: nearly 30% of the sense siRNA strand was converted to single strand after 1 hr incubation, but no single-stranded anti-sense strand was detected (Figure 1D, siRNA E).

We calculated the stability of the initial four base pairs of the siRNA strands in Figure 1 using the nearest-neighbor method and the mfold algorithm (Mathews et al., 1999; Zuker, 2003). The 5′ end of the sense siRNA strand in Figure 1E, but not that in Figure 1B, is predicted to exist as an equilibrium of two conformers of nearly equal energy. In one conformer, the 5′ nucleotide of the sense strand is bound to the anti-sense strand by a U:G wobble pair, whereas in the other conformer the 5′ end of this siRNA strand is unpaired (Supplemental Figures S1A–S1C online at http://www.cell.com/cgi/content/full/115/2/199/DC1). The analysis suggests that RISC assembly favors the siRNA strand whose 5′ end has a greater propensity to fray.

To test our hypothesis, we examined the strand-specific rates of cleavage of sense and anti-sense human *Cu, Zn-superoxide dismutase* (*sod1*) RNA targets (Figure 2A) triggered by the siRNA duplexes shown in Figure 2. In Figure 2B, the 5′ ends of both siRNA strands of the duplex are in G:C base pairs, and the two strands are similar in their rates of target cleavage. In Figure 2C, the C at position 19 of the sense strand was changed to A, causing the anti-sense strand to begin with an unpaired nucleotide. This change, which was made to the sense-strand of the siRNA, caused the rate of target cleavage guided by the anti-sense siRNA strand to be dramatically enhanced and the sense strand rate to be suppressed (Figure 2C). Because the enhancement of sense target cleavage was caused by a mutation in the sense siRNA strand, which does not participate in the recognition of this target, the effect of the mutation must be on a step in the RNAi pathway that is spatially or temporally coupled to siRNA unwinding. However, the suppression of anti-sense target cleavage might have resulted from the single-nucleotide mismatch between the sense strand and its target RNA generated by the C-to-U substitution.

To exclude this possibility, we used a different strategy to unpair the 5′ end of the anti-sense strand. In Figure 2D, the sense strand is identical to that in Figure 2B, but the first nucleotide of the anti-sense strand was changed from G to U, creating a U-C mismatch at its 5′ end in place of the G-A of Figure 2C. This siRNA duplex still showed pronounced asymmetry, with the anti-sense strand guiding target cleavage to the nearly complete exclusion of the sense strand (Figure 2D). Thus, the suppression of the cleavage rate of the sense strand in Figure 2C was not a consequence of the position 19 mismatch with the anti-sense target. This finding is consistent with previous studies that suggest that mismatches with the target RNA are well tolerated if they occur near the 3′ end of the siRNA guide strand (Amarzguioui et al., 2003). When we paired the sense strand of Figure 2C with the anti-sense strand of Figure 2D to create the duplex in Figure 2E, the resulting siRNA directed anti-sense target cleavage significantly better than the siRNA in Figure 2C, although the two siRNAs contain the same sense strand (Figure 2E).

Figures 2F–2H show a similar analysis in which the 5′ end of the sense strand or position 19 of the anti-sense strand of the siRNA in Figure 2B was altered to produce siRNA duplexes in which the 5′ end of the sense strand was either fully unpaired (Figures 2F and 2G) or in an A:U base pair (Figure 2H). Again, unpairing the 5′ end of an siRNA strand—the sense strand in this case—caused that strand to function to the exclusion of the other strand. When the sense strand 5′ end was present in an A:U base pair and the anti-sense strand 5′ end was in a G:C pair, the sense strand dominated the reaction (Figure 2H), but the anti-sense strand retained activity similar to that seen for the original siRNA (Figure 2B). We conclude that the relative ease with which the 5′ ends of the two siRNAs can be liberated from the duplex determines the degree of asymmetry. Additional data supporting this idea is shown in Supplemental Figure S1. Figure S1F shows an siRNA that cleaved the two *sod1* target RNAs (Figure S1D) with modest functional asymmetry that reflects the collective base pairing

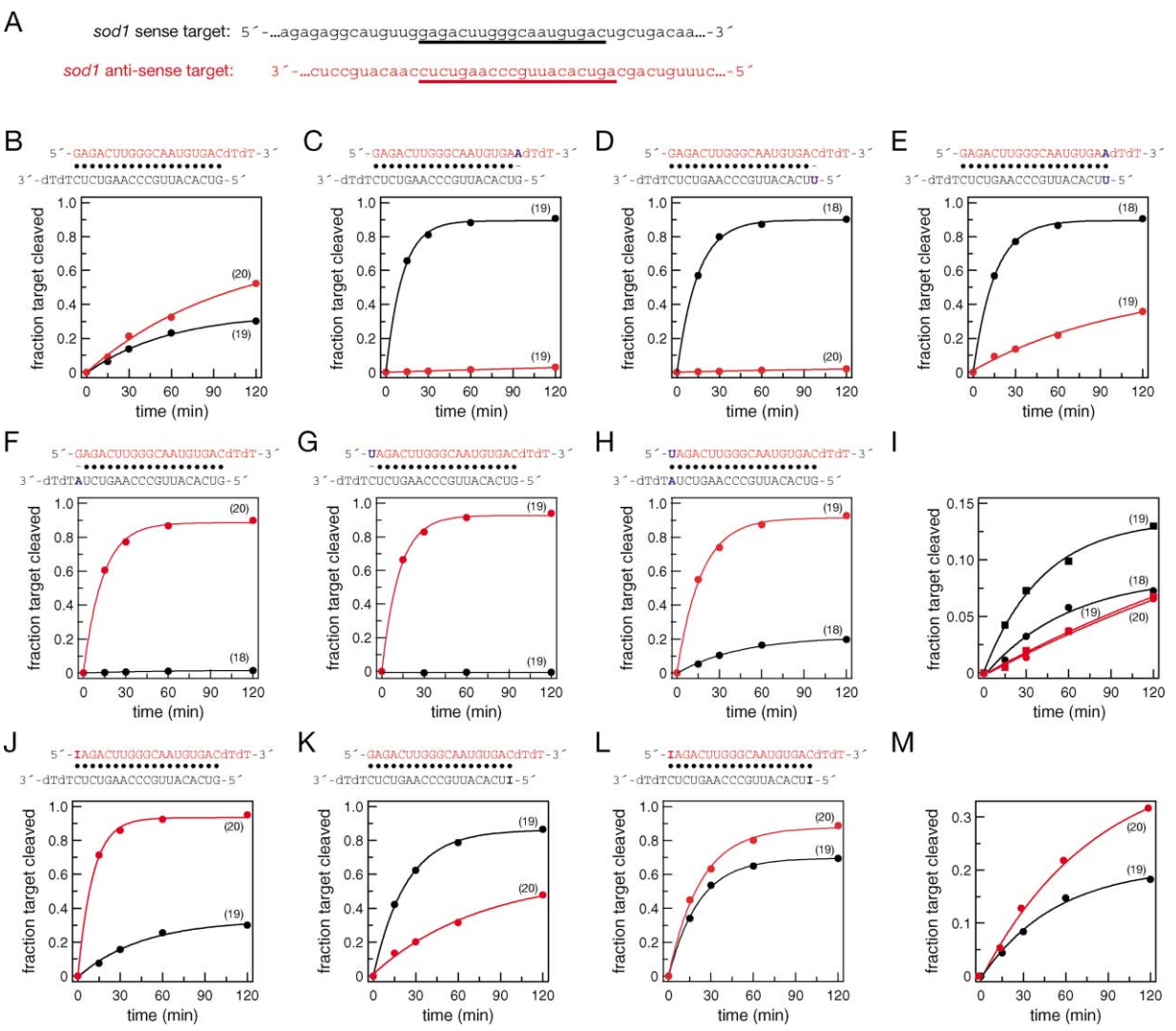

Figure 2. 5′ Terminal, Single-Nucleotide Mismatches Make siRNA Duplexes Functionally Asymmetric

(A) The sequences at the cleavage site of the 560 nt *sod1* RNA sense or 578 nt *sod1* anti-sense target RNAs. The siRNAs in this figure and in Figure 3 cleave the sense target to yield a 320 nt 5′ product and the anti-sense target to yield a 261 nt 5′ product.

(B–H) In vitro RNAi reactions programmed with the siRNA indicated above each graph using the target RNAs diagrammed in (A).

(I) In vitro RNAi reactions programmed with anti-sense or sense single-stranded, 5′ phosphorylated siRNAs (the single nucleotide mismatch with target RNA is underlined): black squares, 5′-pGUCACAUUGCCCAAGUCUCdTdT-3′; black circles, 5′-pUUCACAUUGCCCAAGUCUCdTdT-3′; red squares, 5′-pGAGACUUGGGCAAUGUGAAdTdT-3′; red circles, 5′-pGAGACUUGGGCAAUGUGACdTdT-3′.

(J–M) A single hydrogen bond difference can cause the two strands of an siRNA duplex to assemble differentially into RISC. (J–L) In vitro RNAi reactions programmed with the siRNA indicated above each graph using the target RNAs in (A). (M) In vitro RNAi reactions as in (J)–(L) but programmed with anti-sense or sense single-stranded, 5′ phosphorylated siRNAs: black circles, 5′-IUCACAUUGCCCAAGUCUCdTdT-3′; red circles, 5′-IAGACUUGGGCAAUGUGACdTdT-3′.

strength of the first four nucleotides of each siRNA strand (Figure S1E; see below). Asymmetry was dramatically increased when a G:U wobble was introduced at the 5′ end of the anti-sense strand of the siRNA (Figure S1G), but no asymmetry was seen when the individual single-strands strands were used to trigger RNAi (Figure S1H), demonstrating that differential RISC assembly, not target accessibility, explains the functional asymmetry of the siRNA duplex.

A Single Hydrogen Bond Can Determine Which siRNA Strand Directs RNAi

How small a difference in siRNA base pairing can the RISC-assembly machinery sense? To explore this question, we altered the siRNA in Figure 2B by introducing inosine (I) in place of the initial guanosines of the siRNA strands. These siRNAs cleave the same sites on the two target RNAs as the siRNA in Figure 2B but contain I:C pairs instead of G:C. An I:C pair is similar in energy to an A:U (Turner et al., 1987). When the sense strand began with I, it directed target cleavage more efficiently than the anti-sense strand (Figure 2J). An inosine at the 5′ end of the anti-sense strand had the opposite effect (Figure 2K). Thus, a difference of a single hydrogen bond has a measurable effect on the symmetry of RISC assembly. When both siRNA strands began with I, the relative efficacy of the two siRNA strands (Figure 2L) was restored to that measured for the individual single

strands (Figure 2M). Thus, the small difference in rates in Figure 2L reflects a difference in the intrinsic capacity of the two strands to guide cleavage, not a difference in their assembly into RISC. We note that the absolute rates are faster for the siRNA in Figure 2L than that in Figure 2B, suggesting that production of RISC from an individual strand is governed not only by the relative propensity of the two 5′ ends to fray, but also by their absolute propensities to fray.

We hypothesize that siRNA end fraying provides an entry site for an ATP-dependent RNA helicase that unwinds siRNA duplexes (Figure 4A). The involvement of a helicase in RISC assembly is supported by previous observations. (1) Both siRNA unwinding and production of functional RISC require ATP in vitro (Nykänen et al., 2001), and (2) several proteins with sequence homology to ATP-dependent RNA helicases have been implicated in RNA silencing (Wu-Scharf et al., 2000; Dalmay et al., 2001; Hutvágner and Zamore, 2002; Ishizuka et al., 2002; Kennerdell et al., 2002; Tabara et al., 2002; Tijsterman et al., 2002). However, other mechanisms are possible, including strand selection by an ATP-dependent nuclease or the concerted action on the siRNA of an ATPase and single-stranded RNA binding proteins and/or nucleases.

Four to six bases of single-stranded nucleic acid are bound by the well-studied helicases PcrA (Velankar et al., 1999) and NS3 (Kim et al., 1998). Therefore, we tested the effect of single-nucleotide mismatches in this region of the siRNA using a series of siRNAs containing a mismatch at the second, third, or fourth position of each siRNA strand. We also analyzed siRNAs bearing G:U wobble pairs at the second, third, or both second and third positions (Figure 3). These siRNAs were again based on the siRNA in Figure 2B and targeted the *sod1* sense and anti-sense RNAs in Figure 2A. The results of this series demonstrate that mismatches, but not G:U wobbles, at positions 2–4 of an siRNA strand alter the relative loading of the two siRNA strands into RISC. Mismatches at position five have very modest effects on the relative loading of the siRNA strands into RISC (data not shown). In contrast, the effects of internal mismatches at positions 6–15 cannot be explained by their influencing the symmetry of RISC assembly (data not shown). In sum, these data are consistent with the action of a nonprocessive helicase that can bind about four nucleotides of RNA.

Implications of siRNA Asymmetry for miRNA Biogenesis

miRNAs are derived from the double-stranded stem of hairpin precursor RNAs by cleavage catalyzed by the double-stranded RNA-specific endonuclease Dicer (Lee et al., 1993; Pasquinelli et al., 2000; Reinhart et al., 2000; Grishok et al., 2001; Hutvágner et al., 2001; Ketting et al., 2001; Lagos-Quintana et al., 2001, 2002; Lau et al., 2001; Lee and Ambros, 2001; Reinhart et al., 2002). Pre-miRNA processing by Dicer may generate a product with the essential structure of an siRNA duplex, as first suggested by Bartel and colleagues (Reinhart et al., 2002; Lim et al., 2003b). Using a small RNA cloning strategy to identify mature miRNAs in *C. elegans*, they recovered small RNAs corresponding to the non-miRNA side of the precursor's stem (Lim et al., 2003b). Although these miRNA* sequences were recovered at about 100 times lower frequency than the miRNAs themselves, they could always be paired with the corresponding miRNA to give miRNA duplexes with 2 nt overhanging 3′ ends (Lim et al., 2003b). Their data suggest that miRNAs are born as duplexes but accumulate as single-strands because some subsequent process stabilizes the miRNA, destabilizes the miRNA*, or both.

We propose that incorporation of miRNA into RISC is this process. Our results with siRNA suggest that preferential assembly of a miRNA into the RISC would be accompanied by destruction of its * strand (Figure 4A). To favor miRNA accumulation, miRNA duplexes would present the miRNA in a structure that loads the miRNA strand, but not the miRNA*, into RISC.

Is this idea plausible? We deduced the miRNA duplex that might be generated by processing of pre-*let-7* ("conceptual dicing," Figure 4B). Pre-miRNA stems are only partially double stranded; the typical animal pre-miRNA contains mismatches, internal loops, and G:U base pairs predicted to distort an RNA helix. As a consequence, miRNA duplexes should also contain terminal and internal mismatches and G:U base pairs. For pre-*let-7*, the 5′ end of *let-7* is unpaired in the predicted miRNA duplex, whereas the 5′ end of the * strand is paired. The results presented in Figures 1 and 2 predict that this structure should cause the *let-7* strand to enter the RISC and the *let-7** strand to be degraded. Emboldened by this thought experiment, we extended the analysis to other *Drosophila* miRNA genes (Lagos-Quintana et al., 2001). For each, we inferred from its precursor structure the double strand predicted to be produced by Dicer. These conceptually diced miRNA duplexes are shown in Figure 4C. For 20 of the 27 duplexes analyzed (including pre-*let-7*), the difference in the base pairing of the first five nucleotides of the miRNA versus the miRNA* strand accurately predicted the miRNA, and not the miRNA*, to accumulate in vivo. The analysis succeeded irrespective of which side of the pre-miRNA stem encoded the mature miRNA. In this analysis, we relied on our observations that single mismatches in the first four nucleotides of an siRNA strand, an initial G:U wobble pair, but not internal G:U wobbles, directed the asymmetric incorporation of an siRNA strand into RISC (Figures 1, 2, 3, and S1). However, our experiments with siRNA predict that both the miRNA and the miRNA* strand should accumulate for miR-2a-2, miR-4, miR-5, one of the three miR-6 paralogs, miR-8, miR-10, and miR-13a. Recently, Tuschl and colleagues reported an exhaustive effort to clone and sequence miRNAs from *Drosophila* (Aravin et al., 2003). They found that miR-2a-2*, miR-4*, miR-8*, miR-10*, and miR-13a* are all expressed in vivo. We have confirmed by Northern hybridization that both miR-10 and miR-10* are expressed in adult *Drosophila* males and females and in syncitial blastoderm embryos (Supplemental Figure S2). Thus, of the seven miRNAs we predict to accumulate as both miRNA and miRNA* species, five have now been confirmed experimentally. No miRNA* species were cloned by Tuschl and colleagues for any of the miRNAs we predicted to accumulate asymmetrically (Aravin et al., 2003). These data strengthen our proposal that pre-miRNAs specify on which side of the stem the miRNA resides by generating miRNA duplexes from which only one of the two strands is assembled into RISC. When these double-stranded miRNA intermediates do not

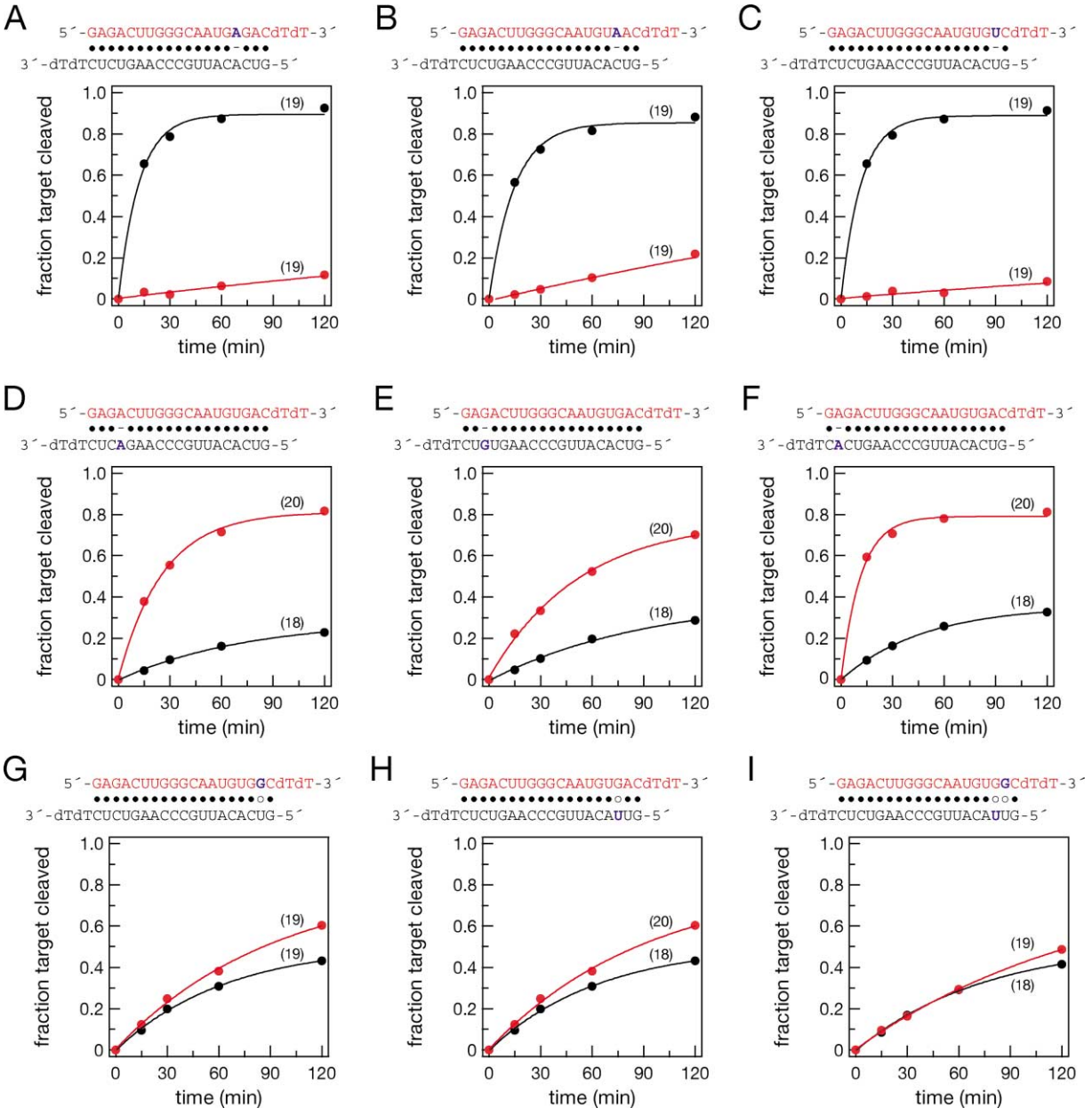

Figure 3. The First Four Base Pairs of the siRNA Duplex Determine Strand-Specific Activity

Internal, single-nucleotide mismatches (A–F) near the 5′ ends of an siRNA strand generate functional asymmetry but internal G:U wobble pairs (G–I) do not. Target RNAs were as in Figure 2A.

contain structural features enforcing asymmetric RISC assembly, both strands accumulate in vivo. It is tempting to speculate that pre-miRNAs such as pre-miR-10, which generates roughly equal amounts of small RNA products from both sides of the precursor stem, regulate target RNAs with partial complementary to either small RNA product.

Implications for RNA Silencing

Our observations have important implications for the design of functional siRNAs for mammalian RNAi. We have shown that siRNA structure can profoundly influence the entry of the anti-sense siRNA strand into the RNAi pathway. A review of the published literature suggests that the structure of the siRNA duplex, rather than that of the target site, explains most reports of ineffective siRNAs duplexes. Such inactive duplexes may be coaxed back to life simply by modifying the *sense* strand of the siRNA. An example of this is shown in Supplemental Figure S1 for an ineffective siRNA directed against the *huntingtin* (*htt*) mRNA (Figure S2K). Changing the G:C (Figure S2K) to an A:U pair (Figure S2L) or a G-A mismatch (Figure S2M) dramatically improved its target cleavage rate in vitro and its efficacy in vivo (E. Milkani, N.A., and P.D.Z., unpublished data). Because RNAi is a natural cellular pathway, siRNAs should be designed to

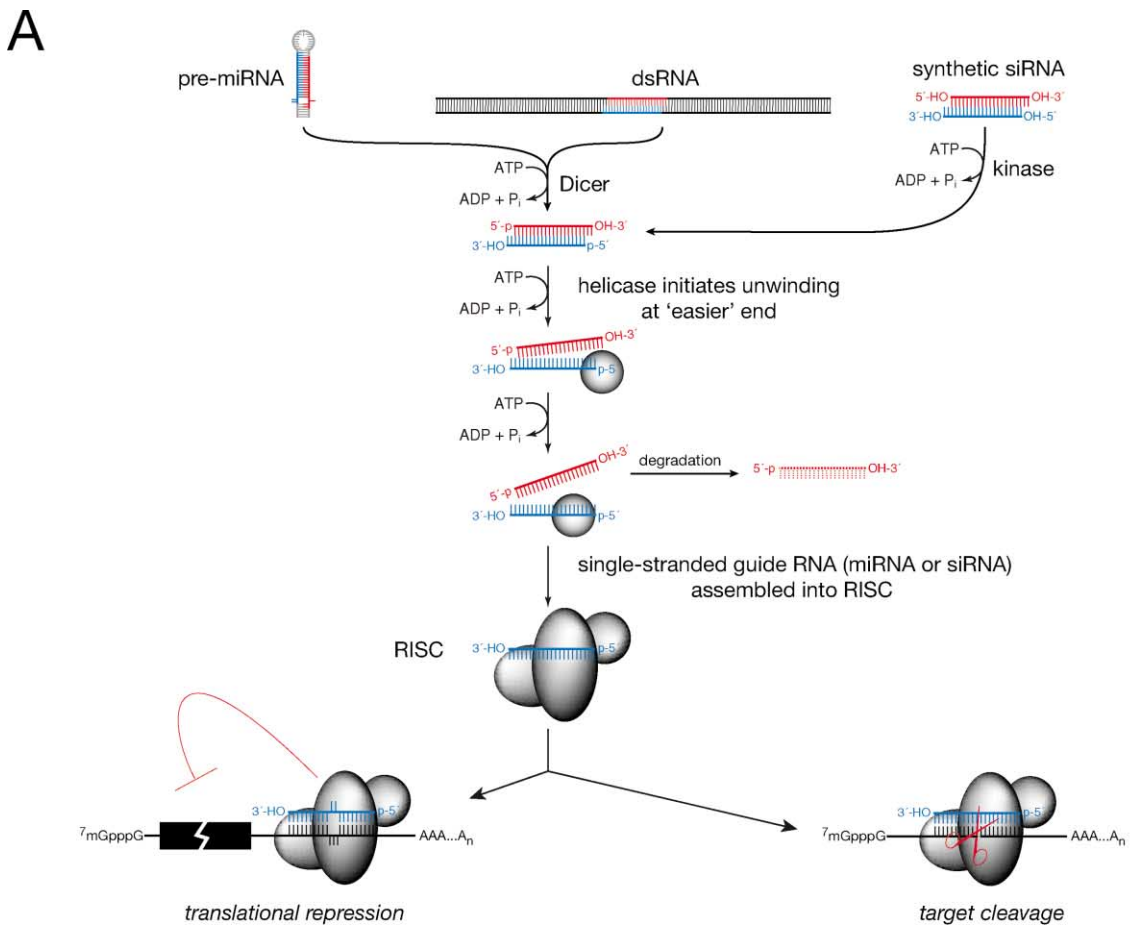

Figure 4. Asymmetric RISC Assembly Can Explain siRNA and miRNA Strand Choice

(A) A model for RISC assembly. Dicing of both pre-miRNAs and dsRNA is proposed to generate a duplex intermediate that is a substrate for an ATP-dependent RNA helicase that directs only one of the two strands into RISC; the other strand is degraded.

(B and C) Asymmetric RISC assembly from double-stranded intermediates explains why miRNAs accumulate in vivo as single strands. (B) pre-*let-7* might be processed by Dicer into a miRNA duplex in which the 5′ end of *let-7*, but not that of *let-7**, is unpaired. (C) The miRNA duplexes predicted to result from Dicer cleavage of *Drosophila* miRNA precursors. The end bearing features predicted to promote asymmetric siRNA strand incorporation into RISC is highlighted in yellow, and the mature miRNA sequence is in italics. Analysis of the predicted miR-10/miR-10* duplex, for which both ends are highlighted in purple, provides little information as to why miR-10 would predominate in vivo. miRNA sequences are from Lagos-Quintana et al. (2001) and Brennecke et al. (2003), with minor sequence corrections from Aravin et al. (2003); miRNA* sequences for miR-2a-2, miR-4, miR-8, miR-10, and miR-13a are as reported by Aravin et al. (2003).

reflect the biological requirements for entry of the anti-sense strand into RISC. In cultured HeLa cells, siRNAs designed according to the mechanism-based rules presented in this paper show maximum suppression of target mRNA expression at concentrations ~100-fold lower than those typically used in mammalian RNAi studies (Schwarz et al., 2002, and our unpublished data). Rana and colleagues previously noted the disproportionate influence of the 5′ nucleotides of the anti-sense strand on siRNA function (Chiu and Rana, 2003). Consistent with our in vitro data, Khvorova and colleagues have found that a low base-pairing stability at the 5′ end of the anti-sense strand, but not the sense strand, characterizes functional siRNAs in cultured cells (Khvorova et al., 2003 [this issue of *Cell*]).

siRNAs designed to function asymmetrically may also be used to enhance RNAi specificity. Expression profiling studies show that the sense strand of an siRNA can direct off-target gene silencing (Jackson et al., 2003). A potential remedy for such sequence-specific but undesirable effects is to redesign the siRNA so that only the anti-sense strand enters the RNAi pathway.

Our observations also suggest a need to revise the current design rules for the construction of short hairpin RNA (shRNA) vectors, which produce siRNAs transcriptionally in cultured cells or in vivo (Brummelkamp et al., 2002; McManus et al., 2002; Paddison et al., 2002; Paul et al., 2002; Sui et al., 2002; Yu et al., 2002). We suggest that shRNAs be designed to place the 5′ end of the anti-sense siRNA strand in a mismatch or G:U base pair. Moreover, a recent report suggests that some shRNAs may induce the interferon response (Bridge et al., 2003). Mismatches and G:U pairs could be designed into these shRNAs simultaneously to promote entry of the correct siRNA strand into the RNAi pathway and to diminish the capacity of the shRNA stem to trigger nonsequence-specific responses to double-stranded RNA. Redesigning shRNAs to more fully reflect the natural mechanism of miRNA incorporation into RISC should make them more effective, allowing lower levels of shRNA to silence target mRNAs in vivo.

Experimental Procedures

General Methods

In vitro RNAi reactions and analysis was carried out as previously described (Tuschl et al., 1999; Zamore et al., 2000; Haley et al., 2003). Target RNAs were used at ~5 nM concentration so that reactions were mainly under single-turnover conditions. Target cleavage under these conditions was proportionate to siRNA concentration. siRNA unwinding assays were as published (Nykänen et al., 2001).

siRNA Preparation

Synthetic RNA (Dharmacon) was deprotected according to the manufacturer's protocol. siRNA strands were annealed (Elbashir et al., 2001a) and used at a final concentration of ≤50 (Figures 1B, 2, 3, and Supplemental Figures S1F–S1H) or ≤100 nM (Figures 1D, 1E, and Supplemental Figures S1K–S1M). siRNA single strands were phosphorylated with polynucleotide kinase (PNK; New England Biolabs) and 1 mM ATP and used at 500 nM final concentration.

Target RNA Preparation

Target RNAs were transcribed with recombinant histidine-tagged T7 RNA polymerase from PCR products as described (Nykänen et al., 2001; Hutvágner and Zamore, 2002) except for sense *sod1* mRNA, which was transcribed from a plasmid template (Crow et al., 1997) linearized with BamHI. PCR templates for *htt* sense and anti-sense and *sod1* anti-sense target RNAs were generated by amplifying 0.1 ng/μl (final concentration) plasmid template encoding *htt* or *sod1* cDNA using the following primer pairs: *htt* sense target, 5′-GCGTAATACGACTCACTATAGGAACAGTATGTCTCAGACATC-3′ and 5′-UUCGAAGUAUUCCGCGUACGU-3′; *htt* anti-sense target, 5′-GCGTAATACGACTCACTATAGGACAAGCCTAATTAGTGATGC-3′ and 5′-GAACAGTATGTCTCAGACATC-3′; *sod1* anti-sense target, 5′-GCGTAATACGACTCACTATAGGGCTTTGTTAGCAGCCGGAT-3′ and 5′-GGGAGACCACAACGGTTTCCC-3′.

Immobilized 2′-*O*-methyl Oligonucleotide Capture of RISC

The 5′ end of the siRNA strand to be measured was ^{32}P-radiolabeled with PNK. 10 pmol biotinylated 2′-*O*-Methyl RNA was immobilized on Dynabeads M280 (Dynal) by incubation in 10 μl lysis buffer containing 2 mM DTT for 1 hr on ice with the equivalent of 50 μl of the suspension of beads provided by the manufacturer. The beads were then washed to remove unbound oligonucleotide. 50 nM siRNA was preincubated in a standard 50 μl in vitro RNAi reaction for 15 min at 25°C. Then, all of the immobilized 2′-*O*-Methyl oligonucleotide was added to the reaction and the incubation continued for 1 hr at 25°C. After incubation, the beads were rapidly washed three times with lysis buffer containing 0.1% (w/v) NP-40 and 2 mM DTT followed by a wash with the same buffer without NP-40. Input and bound radioactivity were determined by scintillation counting (Beckman). The 5′-biotin moiety was linked via a six-carbon spacer arm. 2′-*O*-methyl oligonucleotides (IDT) were: 5′-biotin-ACAUUUCGAAGUAU UCCGCGUACGUGAUGUU-3′ (to capture the siRNA sense strand) and 5′-biotin-CAUCACGUACGCGGAAUACUUCGAAAUGUCC-3′ (to capture the anti-sense strand).

Acknowledgments

We thank Martin Simard for noting the unpaired end of *let-7* in pre-*let-7*; Steve Blacklow and Barbara Golden for suggesting we use inosine to test siRNA asymmetry; Natasha Caplen, Tom Tuschl, and Anastasia Khvorova for sharing data before publication; Eftim Milkani for help preparing Figure 4; Juanita McLachlan for preparing lysates and maintaining our fly colony; and David Bartel, Craig Mello, Tariq Rana, and members of the Zamore lab for encouragement, helpful discussions, and comments on the manuscript. Most importantly, we thank Doug Turner for patiently teaching us to calculate theoretical free energies. G.H. is a Charles A. King Trust fellow of the Medical Foundation. P.D.Z. is a Pew Scholar in the Biomedical Sciences and a W.M. Keck Foundation Young Scholar in Medical Research. This work was supported in part by grants from the National Institutes of Health to P.D.Z. (GM62862-01 and GM65236-01), to N.A. (R01 NS38194), and to Z.X. and P.D.Z. (R21 NS44952-01), and by a grant from the Hereditary Disease Foundation to N.A. and P.D.Z.

Received: June 18, 2003
Revised: August 22, 2003
Accepted: September 12, 2003
Published: October 16, 2003

References

Amarzguioui, M., Holen, T., Babaie, E., and Prydz, H. (2003). Tolerance for mutations and chemical modifications in a siRNA. Nucleic Acids Res. *31*, 589–595.

Ambros, V., Bartel, B., Bartel, D.P., Burge, C.B., Carrington, J.C., Chen, X., Dreyfuss, G., Eddy, S.R., Griffiths-Jones, S., Marshall, M., et al. (2003). A uniform system for microRNA annotation. RNA *9*, 277–279.

Aravin, A.A., Lagos-Quintana, M., Yalcin, A., Zavolan, M., Marks, D., Snyder, B., Gaasterland, T., Meyer, J., and Tuschl, T. (2003). The small RNA profile during Drosophila melanogaster development. Dev. Cell *5*, 337–350.

Bernstein, E., Caudy, A.A., Hammond, S.M., and Hannon, G.J. (2001). Role for a bidentate ribonuclease in the initiation step of RNA interference. Nature *409*, 363–366.

Billy, E., Brondani, V., Zhang, H., Muller, U., and Filipowicz, W. (2001). Specific interference with gene expression induced by long, double-stranded RNA in mouse embryonal teratocarcinoma cell lines. Proc. Natl. Acad. Sci. USA *98*, 14428–14433.

Boutla, A., Delidakis, C., Livadaras, I., Tsagris, M., and Tabler, M. (2001). Short 5′-phosphorylated double-stranded RNAs induce RNA interference in *Drosophila*. Curr. Biol. *11*, 1776–1780.

Brennecke, J., Hipfner, D.R., Stark, A., Russell, R.B., and Cohen, S.M. (2003). bantam encodes a developmentally regulated microRNA that controls cell proliferation and regulates the proapoptotic gene hid in *Drosophila*. Cell *113*, 25–36.

Bridge, A.J., Pebernard, S., Ducraux, A., Nicoulaz, A.L., and Iggo, R. (2003). Induction of an interferon response by RNAi vectors in mammalian cells. Nat. Genet. *34*, 263–264.

Brummelkamp, T.R., Bernards, R., and Agami, R. (2002). A system for stable expression of short interfering RNAs in mammalian cells. Science *296*, 550–553.

Catalanotto, C., Azzalin, G., Macino, G., and Cogoni, C. (2002). Involvement of small RNAs and role of the qde genes in the gene silencing pathway in Neurospora. Genes Dev. *16*, 790–795.

Caudy, A.A., Myers, M., Hannon, G.J., and Hammond, S.M. (2002). Fragile X-related protein and VIG associate with the RNA interference machinery. Genes Dev. *16*, 2491–2496.

Chiu, Y., and Rana, T.M. (2003). siRNA function in RNAi: a chemical modification analysis. RNA *9*, 1034–1048.

Chiu, Y.-L., and Rana, T.M. (2002). RNAi in human cells: basic structural and functional features of small interfering RNA. Mol. Cell *10*, 549–561.

Crow, J.P., Sampson, J.B., Zhuang, Y., Thompson, J.A., and Beckman, J.S. (1997). Decreased zinc affinity of amyotrophic lateral sclerosis-associated superoxide dismutase mutants leads to enhanced catalysis of tyrosine nitration by peroxynitrite. J. Neurochem. *69*, 1936–1944.

Dalmay, T., Horsefield, R., Braunstein, T.H., and Baulcombe, D.C. (2001). SDE3 encodes an RNA helicase required for post-transcriptional gene silencing in Arabidopsis. EMBO J. *20*, 2069–2078.

Doench, J.G., Petersen, C.P., and Sharp, P.A. (2003). siRNAs can function as miRNAs. Genes Dev. *17*, 438–442.

Doi, N., Zenno, S., Ueda, R., Ohki-Hamazaki, H., Ui-Tei, K., and Saigo, K. (2003). Short-interfering-RNA-mediated gene silencing in mammalian cells requires Dicer and eIF2C translation initiation factors. Curr. Biol. *13*, 41–46.

Elbashir, S.M., Lendeckel, W., and Tuschl, T. (2001a). RNA interference is mediated by 21- and 22-nucleotide RNAs. Genes Dev. *15*, 188–200.

Elbashir, S.M., Martinez, J., Patkaniowska, A., Lendeckel, W., and Tuschl, T. (2001b). Functional anatomy of siRNAs for mediating efficient RNAi in Drosophila melanogaster embryo lysate. EMBO J. *20*, 6877–6888.

Fire, A., Xu, S., Montgomery, M.K., Kostas, S.A., Driver, S.E., and Mello, C.C. (1998). Potent and specific genetic interference by double-stranded RNA in Caenorhabditis elegans. Nature *391*, 806–811.

Grishok, A., Pasquinelli, A.E., Conte, D., Li, N., Parrish, S., Ha, I., Baillie, D.L., Fire, A., Ruvkun, G., and Mello, C.C. (2001). Genes and mechanisms related to RNA interference regulate expression of the small temporal RNAs that control *C. elegans* developmental timing. Cell *106*, 23–34.

Haley, B., Tang, G., and Zamore, P.D. (2003). In vitro analysis of RNA interference in Drosophila melanogaster. Methods *30*, 330–336.

Hamilton, A.J., and Baulcombe, D.C. (1999). A species of small antisense RNA in posttranscriptional gene silencing in plants. Science *286*, 950–952.

Hammond, S.M., Bernstein, E., Beach, D., and Hannon, G.J. (2000). An RNA-directed nuclease mediates post-transcriptional gene silencing in Drosophila cells. Nature *404*, 293–296.

Hammond, S.M., Caudy, A.A., and Hannon, G.J. (2001). Post-transcriptional gene silencing by double-stranded RNA. Nat. Rev. Genet. *2*, 110–119.

Hutvágner, G., and Zamore, P.D. (2002). A MicroRNA in a Multiple-Turnover RNAi Enzyme Complex. Science *297*, 2056–2060.

Hutvágner, G., McLachlan, J., Pasquinelli, A.E., Balint, É., Tuschl, T., and Zamore, P.D. (2001). A cellular function for the RNA-interference enzyme Dicer in the maturation of the let-7 small temporal RNA. Science *293*, 834–838.

Ishizuka, A., Siomi, M.C., and Siomi, H. (2002). A Drosophila fragile X protein interacts with components of RNAi and ribosomal proteins. Genes Dev. *16*, 2497–2508.

Jackson, A.L., Bartz, S.R., Schelter, J., Kobayashi, S.V., Burchard, J., Mao, M., Li, B., Cavet, G., and Linsley, P.S. (2003). Expression profiling reveals off-target gene regulation by RNAi. Nat. Biotechnol. *21*, 635–637.

Kennerdell, J.R., Yamaguchi, S., and Carthew, R.W. (2002). RNAi is activated during Drosophila oocyte maturation in a manner dependent on aubergine and spindle-E. Genes Dev. *16*, 1884–1889.

Ketting, R.F., Fischer, S.E., Bernstein, E., Sijen, T., Hannon, G.J., and Plasterk, R.H. (2001). Dicer functions in RNA interference and in synthesis of small RNA involved in developmental timing in C. elegans. Genes Dev. *15*, 2654–2659.

Khvorova, A., Reynolds, A., and Jayasena, S.D. (2003). Functional siRNAs and miRNAs exhibit strand bias. Cell *115*, this issue, 209–216.

Kim, J.L., Morgenstern, K.A., Griffith, J.P., Dwyer, M.D., Thomson, J.A., Murcko, M.A., Lin, C., and Caron, P.R. (1998). Hepatitis C virus NS3 RNA helicase domain with a bound oligonucleotide: the crystal structure provides insights into the mode of unwinding. Structure *6*, 89–100.

Knight, S.W., and Bass, B.L. (2001). A role for the RNase III enzyme DCR-1 in RNA interference and germ line development in Caenorhabditis elegans. Science *293*, 2269–2271.

Lagos-Quintana, M., Rauhut, R., Lendeckel, W., and Tuschl, T. (2001). Identification of novel genes coding for small expressed RNAs. Science *294*, 853–858.

Lagos-Quintana, M., Rauhut, R., Yalcin, A., Meyer, J., Lendeckel, W., and Tuschl, T. (2002). Identification of tissue-specific microRNAs from mouse. Curr. Biol. *12*, 735–739.

Lagos-Quintana, M., Rauhut, R., Meyer, J., Borkhardt, A., and Tuschl, T. (2003). New microRNAs from mouse and human. RNA *9*, 175–179.

Lau, N.C., Lim, L.P., Weinstein, E.G., and Bartel, D.P. (2001). An sbundant class of tiny RNAs with probable regulatory roles in *Caenorhabditis elegans*. Science *294*, 858–862.

Lee, R.C., and Ambros, V. (2001). An extensive class of small RNAs in Caenorhabditis elegans. Science *294*, 862–864.

Lee, R.C., Feinbaum, R.L., and Ambros, V. (1993). The C. elegans heterochronic gene lin-4 encodes small RNAs with antisense complementarity to lin-14. Cell *75*, 843–854.

Lim, L.P., Glasner, M.E., Yekta, S., Burge, C.B., and Bartel, D.P. (2003a). Vertebrate microRNA genes. Science *299*, 1540.

Lim, L.P., Lau, N.C., Weinstein, E.G., Abdelhakim, A., Yekta, S., Rhoades, M.W., Burge, C.B., and Bartel, D.P. (2003b). The microRNAs of Caenorhabditis elegans. Genes Dev. *17*, 991–1008.

Mallory, A.C., Reinhart, B.J., Bartel, D., Vance, V.B., and Bowman, L.H. (2002). A viral suppressor of RNA silencing differentially regulates the accumulation of short interfering RNAs and micro-RNAs in tobacco. Proc. Natl. Acad. Sci. USA *99*, 15228–15233.

Martinez, J., Patkaniowska, A., Urlaub, H., Lührmann, R., and Tuschl, T. (2002). Single-stranded antisense siRNAs guide target RNA cleavage in RNAi. Cell *110*, 563–574.

Mathews, D.H., Sabina, J., Zuker, M., and Turner, D.H. (1999). Expanded sequence dependence of thermodynamic parameters improves prediction of RNA secondary structure. J. Mol. Biol. *288*, 911–940.

McManus, M.T., Petersen, C.P., Haines, B.B., Chen, J., and Sharp, P.A. (2002). Gene silencing using micro-RNA designed hairpins. RNA *8*, 842–850.

Mourelatos, Z., Dostie, J., Paushkin, S., Sharma, A.K., Charroux, B., Abel, L., Rappsilber, J., Mann, M., and Dreyfuss, G. (2002). miRNPs: a

novel class of ribonucleoproteins containing numerous microRNAs. Genes Dev. *16*, 720–728.

Myers, J.W., Jones, J.T., Meyer, T., and Ferrell, J.E. (2003). Recombinant Dicer efficiently converts large dsRNAs into siRNAs suitable for gene silencing. Nat. Biotechnol. *21*, 324–328.

Nykänen, A., Haley, B., and Zamore, P.D. (2001). ATP requirements and small interfering RNA structure in the RNA interference pathway. Cell *107*, 309–321.

Paddison, P.J., Caudy, A.A., Bernstein, E., Hannon, G.J., and Conklin, D.S. (2002). Short hairpin RNAs (shRNAs) induce sequence-specific silencing in mammalian cells. Genes Dev. *16*, 948–958.

Park, W., Li, J., Song, R., Messing, J., and Chen, X. (2002). CARPEL FACTORY, a Dicer homolog, and HEN1, a novel protein, act in microRNA metabolism in *Arabidopsis thaliana*. Curr. Biol. *12*, 1484–1495.

Pasquinelli, A.E., Reinhart, B.J., Slack, F., Martindale, M.Q., Kuroda, M.I., Maller, B., Hayward, D.C., Ball, E.E., Degnan, B., Muller, P., et al. (2000). Conservation of the sequence and temporal expression of let-7 heterochronic regulatory RNA. Nature *408*, 86–89.

Paul, C.P., Good, P.D., Winer, I., and Engelke, D.R. (2002). Effective expression of small interfering RNA in human cells. Nat. Biotechnol. *20*, 505–508.

Provost, P., Dishart, D., Doucet, J., Frendewey, D., Samuelsson, B., and Radmark, O. (2002). Ribonuclease activity and RNA binding of recombinant human Dicer. EMBO J. *21*, 5864–5874.

Reinhart, B.J., Slack, F.J., Basson, M., Pasquinelli, A.E., Bettinger, J.C., Rougvie, A.E., Horvitz, H.R., and Ruvkun, G. (2000). The 21-nucleotide let-7 RNA regulates developmental timing in Caenorhabditis elegans. Nature *403*, 901–906.

Reinhart, B.J., Weinstein, E.G., Rhoades, M.W., Bartel, B., and Bartel, D.P. (2002). MicroRNAs in plants. Genes Dev. *16*, 1616–1626.

Schwarz, D.S., Hutvágner, G., Haley, B., and Zamore, P.D. (2002). Evidence that siRNAs function as guides, not primers, in the *Drosophila* and human RNAi pathways. Mol. Cell *10*, 537–548.

Sijen, T., Fleenor, J., Simmer, F., Thijssen, K.L., Parrish, S., Timmons, L., Plasterk, R.H., and Fire, A. (2001). On the role of RNA amplification in dsRNA-triggered gene silencing. Cell *107*, 465–476.

Sui, G., Soohoo, C., Affar el, B., Gay, F., Shi, Y., and Forrester, W.C. (2002). A DNA vector-based RNAi technology to suppress gene expression in mammalian cells. Proc. Natl. Acad. Sci. USA *99*, 5515–5520.

Tabara, H., Yigit, E., Siomi, H., and Mello, C.C. (2002). The dsRNA binding protein RDE-4 interacts with RDE-1, DCR-1, and a DexH-box helicase to direct RNAi in *C. elegans*. Cell *109*, 861–871.

Tang, G., Reinhart, B.J., Bartel, D.P., and Zamore, P.D. (2003). A biochemical framework for RNA silencing in plants. Genes Dev. *17*, 49–63.

Tijsterman, M., Ketting, R.F., Okihara, K.L., Sijen, T., and Plasterk, R.H. (2002). RNA helicase MUT-14-dependent gene silencing triggered in C. elegans by short antisense RNAs. Science *295*, 694–697.

Turner, D.H., Sugimoto, N., Kierzek, R., and Dreiker, S.D. (1987). Free energy increments for hydrogen bonds in nucleic acid base pairs. J. Am. Chem. Soc. *109*, 3783–3785.

Tuschl, T., Zamore, P.D., Lehmann, R., Bartel, D.P., and Sharp, P.A. (1999). Targeted mRNA degradation by double-stranded RNA in vitro. Genes Dev. *13*, 3191–3197.

Velankar, S.S., Soultanas, P., Dillingham, M.S., Subramanya, H.S., and Wigley, D.B. (1999). Crystal structures of complexes of PcrA DNA helicase with a DNA substrate indicate an inchworm mechanism. Cell *97*, 75–84.

Wu-Scharf, D., Jeong, B., Zhang, C., and Cerutti, H. (2000). Transgene and transposon silencing in Chlamydomonas reinhardtii by a DEAH-box RNA helicase. Science *290*, 1159–1163.

Yu, J.Y., DeRuiter, S.L., and Turner, D.L. (2002). RNA interference by expression of short-interfering RNAs and hairpin RNAs in mammalian cells. Proc. Natl. Acad. Sci. USA *99*, 6047–6052.

Zamore, P.D., Tuschl, T., Sharp, P.A., and Bartel, D.P. (2000). RNAi: double-stranded RNA directs the ATP-dependent cleavage of mRNA at 21 to 23 nucleotide intervals. Cell *101*, 25–33.

Zeng, Y., Yi, R., and Cullen, B.R. (2003). MicroRNAs and small interfering RNAs can inhibit mRNA expression by similar mechanisms. Proc. Natl. Acad. Sci. USA *100*, 9779–9784.

Zhang, H., Kolb, F.A., Brondani, V., Billy, E., and Filipowicz, W. (2002). Human Dicer preferentially cleaves dsRNAs at their termini without a requirement for ATP. EMBO J. *21*, 5875–5885.

Zuker, M. (2003). Mfold web server for nucleic acid folding and hybridization prediction. Nucleic Acids Res. *31*, 1–10.